Silicon Mechanical Sensors for High-Temperature Control Systems.
Creation of Samples of Small-Size Pressure and Low-Frequency Acceleration Sensors.

Michael Tikhomirov
1989

For rocket propulsion test systems designed for reusable complexes, there is a lack of means of obtaining information about mechanical parameters. In many cases, test conditions require information about processes and objects when the ambient temperature changes in the range of $0 - 300^{\circ}$C.

Obtaining accurate information on pressure fields is considered a problem. The range of measured pressures is from $0 \div 0.01$ MPa to $0 \div 1$ MPa. The intrinsic error of the sensor should not exceed $\pm 1\%$.

The second problem is to obtain accurate information about the parameters of dynamic stability, dynamic overloads on nodes, and force elements for strength assessment, as well as vibration modes of devices and systems. Range of measured accelerations from $0 \pm 10g$ to $0 \pm 30g$. Frequency spectrum $(0 \div 300)$ Hz. The intrinsic error of the LF accelerometer is less than $\pm 5\%$.

Important requirements for test execution conditions are considered to be the lowest level of perturbation of mechanical impacts by the system elements on the conditions in the units and the ability to obtain information about processes and objects when the ambient temperature changes in the range $\mathbf{(0 \div 300)^{\circ}C}$. To solve such problems, high-temperature sensors are needed with a total dimension of 15 $mm \times 15$ $mm \times 15$ mm and a weight of less than 10 grams.

Based on the results of the studies stated earlier in Chapter 2 and Chapter 3, the designs were designed, prototypes were made, and metrological characteristics of small pressure and acceleration sensors, the appearance of which is shown in Fig.37 and 38, were investigated for unit test systems.

1. Small-Sized High-Temperature Pressure Sensors

The sensors are designed to measure static and dynamic pressure from $0 \div 1$ atm to $0 \div 10$ atm at ambient temperatures (air, oxygen, naphthyl, etc.) in the range of $(0 \div 300)^{\circ}C$.

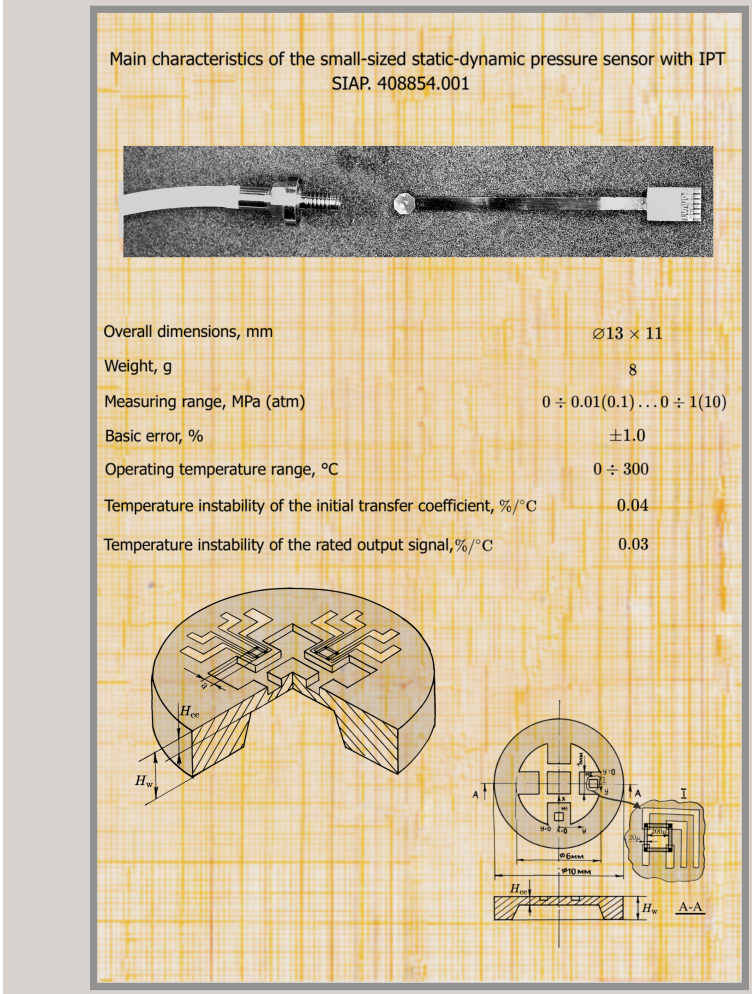

Figure 37. Static-dynamic pressure sensor

Fig.37 shows the sensors and the developed IPT_P SIAP 408 854.001. The IPT_P design incorporates the technical solution of Yu.M. Spalek outlined in [1]. The monolithic silicon structure $EE-RB$ is made in the form of a rigidly fixed plate containing stiffening ribs in the form of rectangular beams.

Such a $EE-RB$ structure (in contrast to a flat rigidly fixed plate) is characterized by less nonlinearity of the transformation characteristic in the range of small pressures.

Piezoresistors MC with distributed parameters are located on the stiffening ribs. The following topological structure was used in IPT_P. Equal contact areas with side sizes $b_c = 20 \cdot 10^{-4}\ cm$, with centers at the vertices of a square with side sizes $a = 200 \cdot 10^{-4}\ cm$, are connected to each other by four piezoresistive single-channel channels with ion-implanted single channels $p-type$ with a width of $d_{ch} = 20 \cdot 10^{-4}\ cm$, oriented along the crystallographic direction [110].

In calculating IPT_P, the temperature changes $R_{in}(T)$ and $K_{ch}(T)$ were determined by the dependences (77) and (19), where K_A, K_B, and K_C of Table 4.1 are equal to $K_A = 10$, $K_B = 60$ and $K_C = -14$. The temperature dependence of the specific resistance for KDB-1.0 plates (material EE) does not have sharp drops up to a temperature of $300^{\circ}C$ and at $T_0 = 150^{\circ}\mathrm{C}$ is determined as

$$\rho_{ee}(T) = 2.2\left[1 + 5.2 \cdot 10^{-3}(T - 150) + 8.2 \cdot 10^{-6}(T - 150)^2\right] \quad [\Omega \cdot cm] \quad (85)$$

Using the manufacturing method proposed in [2], batches of model and experimental samples of IPT_P SIAP 408 854.001 were produced in the company P / Ya R-6668. The assembly of small high-temperature sensors was carried out jointly by the enterprises P/Ya A-1891 and P/Ya R-6668.

2. Integral Single-Component Inertial Accelerometer with Piezoresistive Transducer

The principle of operation and construction of the device (an inertial element that performs double differentiation of [elastic] displacement and a resistive element of resistance, made in the form of a monolithic silicon monocrystal) are well known [3]. The new design, shown in Fig.38, improves the metrological and operational characteristics of known devices.

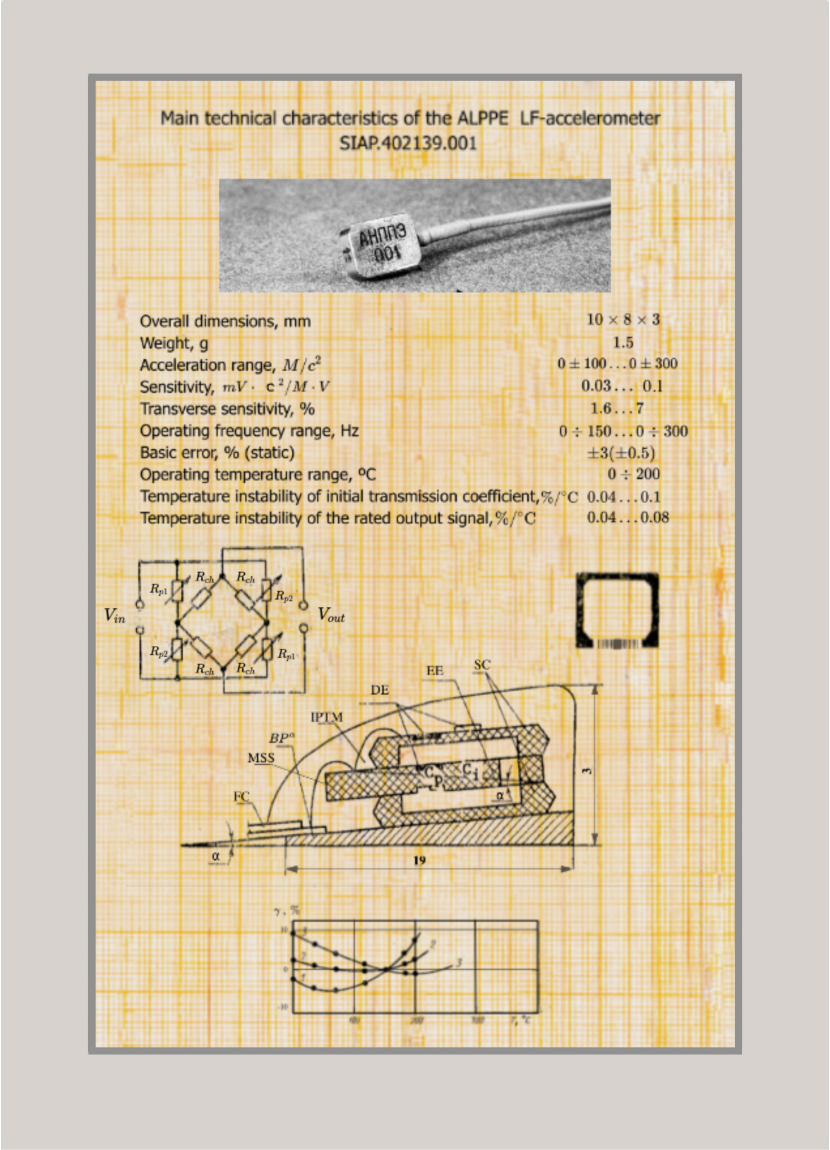

Figura 38. Low-frequency 0-300 acceleration sensors

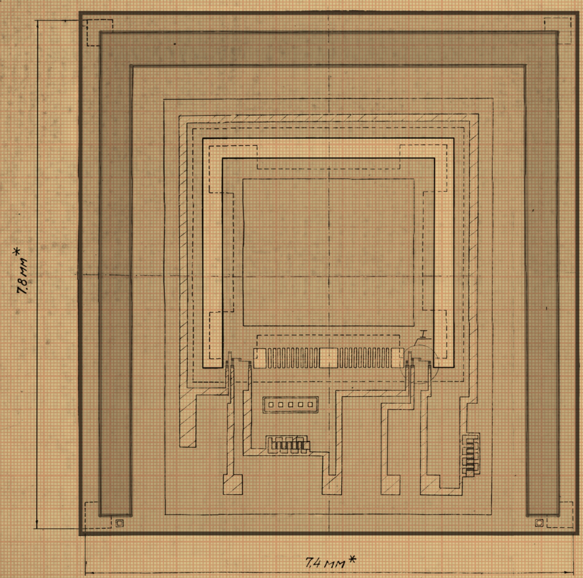

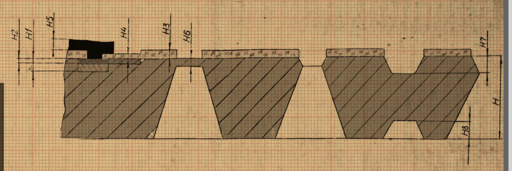

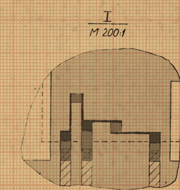

Structure Elements		Thickness, μm	Conductivity Type	Material Used		Drawing Sheet Number
Name	Symbol			Name	GOST (FED-STD), OST (Ind-STD), TS	
Substrate	H	380	n	Silicon wafer, Czochralski grown, 4.5 inch diameter, (100) orientation	GOST 19658-81	
Additional Doping Layer	H1	1,8-2	p^+	Bohr	TS6-02-669-77	2
Ionic-Doped Layer	H2	0,5	p	Bohr	TS6-02-578-72	3
Masking Oxide Layer	H3	0,7±01				
Decanalizing Oxide Layer	H4	0.12				
Metallization Layer	H5	1±0,2		Aluminum A 99	ETO.021 051.Ty	5
Planar Etching Layer (with MSS)	H6	20				9
Etched Seating Layer (planar)	H7	50				11
Etched Seating Layer (unplanar)	H8	50				

1. * Dimensions for reference.
2. Characteristics and data on the manufacture of individual layers are shown in the table.
3. The orientation deviation of the piezoresistors axis relative to the crystallographic direction [011] must be at least 1°.

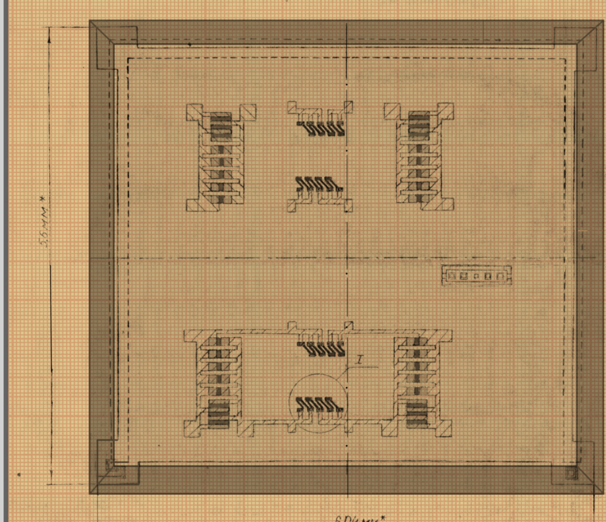

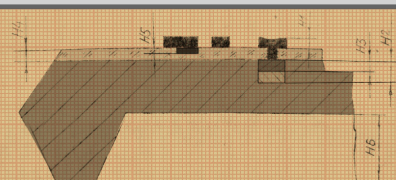

Structure Elements		Thickness, μm	Conductivity Type	Material Used		Drawing Sheet Number
Name	Symbol			Name	GOST (FED-STD), OST (Ind-STD), TS	
Substrate	H	380	n	Silicon wafer, Czochralski grown, 4.5 inch diameter, (100) orientation	GOST 19653-81	
Metallization Layer	H1	1±0,2		Aluminum A 99	ETO.021 051.Ty	1
Additional Doping Layer	H2	2-2,5	p^+	Bohr	TS6-02-669-77	2
Ionic-Doped Layer	H3	0,5	p	Bohr	TS6-02-678-72	3
Decanalizing Oxide Layer	H4	0,7-1				–
RS 1004 Layer	H5	0.05		RS 1004	GOST 23774-79	6
Unplanar Etching Layer	H6	100				9

1. * Dimensions for reference.
2. Characteristics and data on the manufacture of individual layers are shown in the table.

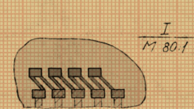

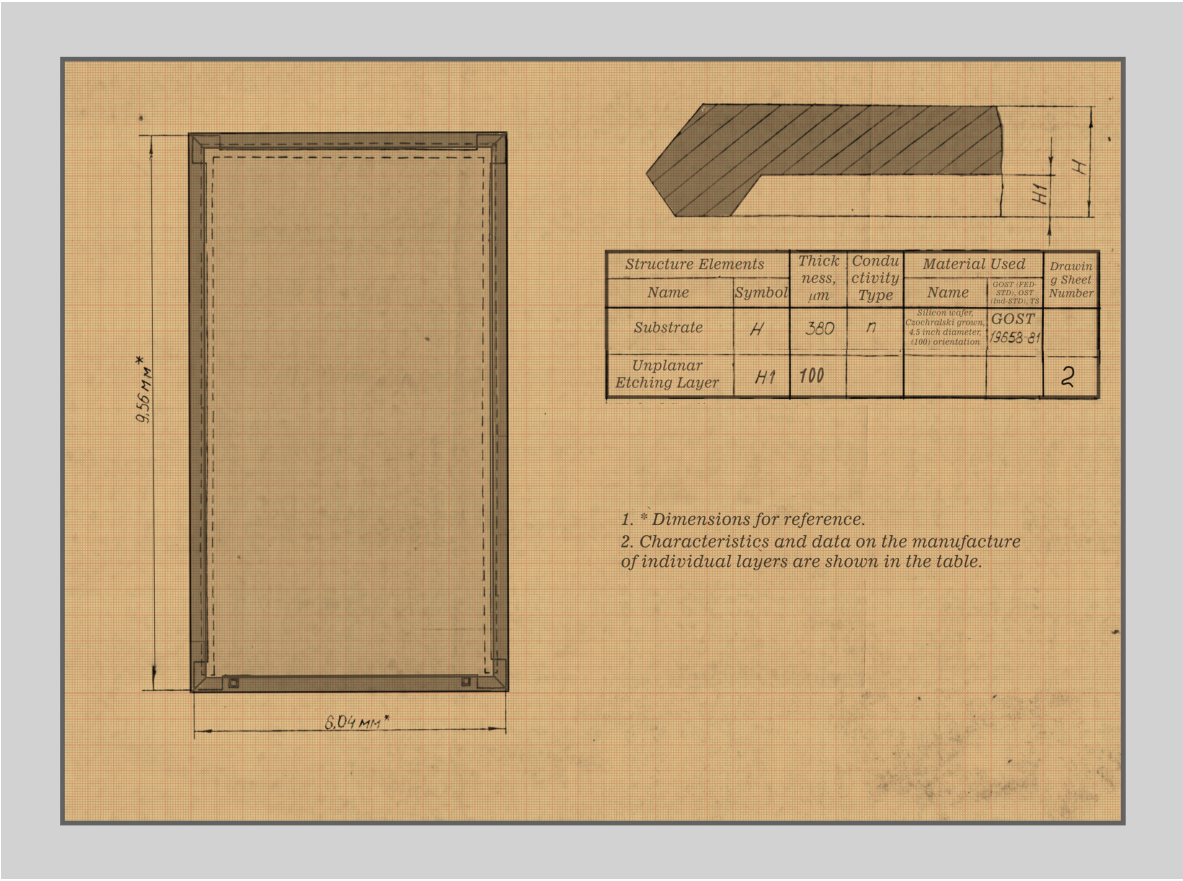

Structure Elements		Thickness, μm	Conductivity Type	Material Used		Drawing Sheet Number
Name	Symbol			Name	GOST (FED-STD, OST (ind-STD), TS	
Substrate	H	380	n	Silicon wafer, Czochralski grown, 4.5 inch diameter, (100) orientation	GOST 19658-81	
Unplanar Etching Layer	H1	100				2

The accelerometer consists of (Fig.38) a measuring module ($IPTM$) installed on a thermal expansion-matched elongation housing (BP^{α}) made of Kovar alloy 29NK. Electrical connection to the next device of the information measurement system is provided by a flexible flat cable (FC) on a polyamide base with an electrical connector RPS1-7. The structural elements (DE) are made of monocrystalline silicon plates oriented in the (100) plane. The elastic element (EE) (see Fig.30) consists of 28 cantilever beams with a length L, width D_i, and thickness H_{ee}, rigidly fixed on a ring support. Resistive elements R_{ch} (or PCH) of the bridge strain gauge circuit (MC) are installed on each of the two beams D_1. The remaining beams D_2, with a total number of beams $\mathrm{n} = 26$, are used to adjust the amplitude characteristics of the conversion (see Chapter 4, Fig.30). Silicon covers (SC) perform the functions of thermocompensating circuits (TCC) and dampers for vibrations of inertial and elastic elements.

The first part of the design, which aims to expand the range of operating temperatures, is associated with the electrical insulation of the piezoresistive element (MC) using a junction $p-n$ in the temperature range up to $200^{\circ}\mathrm{C}$ while maintaining satisfactory conversion characteristics. In this formulation, the insulation failure criterion for MC is defined as a 1% change in sensitivity K_{mc} due to shunting of the output resistance by the elastic element. This criterion can be met by designing MC with a sufficiently small area of the $p-n$ junction. Chapter 4 shows the temperature behavior of the reverse current of the insulating p-junction as a function of the ratio of the perimeter to the surface area of the junction. The option $\#4$ was chosen. Areas of MC were constructed for two options:

- Boron diffusion with average specific resistance values of PCH (where "autocompensation" of temperature changes in sensitivity can be expected in the range of $(0 \div 200)^{\circ}C$ when MC is powered by a stabilized current) of $0.035\ \Omega \cdot cm$;
- For layers modified with ions with a doping dose of $2 \cdot 10^{15}\ cm^{-2}$ ($R_s = 80\ \Omega/\square$).

The second part consists of compensating for the strong influence of temperature on the coefficient of piezoresistive sensitivity without deteriorating the insulation of MC. At temperatures up to $+200^{\circ}\mathrm{C}$, two compensation forms were chosen. One is compensation using the TCC scheme in the power supply circuit located on a separate DE. The second option is compensation of the temperature drift of the current bridge sensitivity, called "autocompensation". Both options are discussed in Chapter 4.

To compensate for the change in accelerometer sensitivity, a circuit (see Figs.31 and 38) is applied, which is constructed as a thermosensitive bridge with two arms with positive TCR and two arms with negative TCR, connected on the diagonal with MC. The arms of the thermosensitive circuit are characterized by the following relationships:

diffusion doping

$$R_{p_1}(T) = R_{p_10}\left[1 + 3.4 \cdot 10^{-3}\left(\mathrm{T} - \mathrm{T}_0\right) + 2.3 \cdot 10^{-6}\left(\mathrm{T} - \mathrm{T}_0\right)^2\right] \quad (86)$$

thin film from $RS1004$

$$R_{p_2}(T) = R_{p_20}\left[1 - 2.7 \cdot 10^{-3}\left(\mathrm{T} - \mathrm{T}_0\right) + 7.3 \cdot 10^{-6}\left(\mathrm{T} - \mathrm{T}_0\right)^2\right] \quad (87)$$

The surface resistance of diffusion-doped layers is $300\ \Omega/\square$, so they can be made with a small area of p-n junctions. The resistor circuit with these characteristics reduces the sensitivity compared to the uncompensated MC by a factor of 1.5 for IPT with ion-doped piezoresistors and by a factor of 1.8 for diffusion-doped piezoresistors.

Self-compensation of IPT powered by a stabilized current is achieved at temperatures of $0 - 200^{\circ}\mathrm{C}$. Fig.38 shows the temperature behavior of the error parameter γ when compensated by the TCC thermistor bridge (curve 2), self-compensation with ion-doped piezoresistive channels (PCH) (curve 3) and diffusion-doped (curve 1). As can be seen in Fig.38, when self-compensating, the error of the accelerometer for both types of IPT does not exceed $0.04\%/^{\circ}\mathrm{C}$.

In a wide range of temperatures, air damping is preferable. For small sensors, damping should be provided in narrow gaps between the planes of the inertial element and the internal surfaces of the housing components SC (covers). In this accelerometer, silicon covers with internal cavities were used. For a specific design, the damping coefficient θ^*, which characterizes the level of damping, is related to the geometric gap size $\mathrm{w} = (20 \div 80) \cdot 10^{-6}\ \mathrm{m}$ by the empirical relationship.

$$\theta^* = \frac{2 \cdot 10^{-11}}{\left(H_{\mathrm{ee}} - 11 \cdot 10^{-6}\right)\left(w - 16 \cdot 10^{-6}\right)}\ , \quad (88)$$

where $\mathrm{H_{ee}} = (15 \div 25) \times 10^{-6}\ \mathrm{m}$ is the thickness of the elastic element.

The mechanical strength of the deformable component of the MSS sensor element is determined by two factors. The first factor is the reduction of geometric dimensions to values corresponding to [4]. The second factor is the treatment of the silicon surface by chemical etching in the process of manufacturing the elastic element [5]. The strength of the elastic element of such a configuration and with such surface treatment is on average 25 times higher than the level of working deformation ($\varepsilon_{\mathrm{x}} = 4 \cdot 10^{-4}$).

Sensitivity adjustment is achieved by destroying strips with a laser. With this method, it is possible to independently adjust sensitivity to the mechanical input parameter and sensitivity to temperature changes. The method is also convenient in that, after adjusting the elastic elements of the entire series of accelerometers for a certain input nominal, they are characterized by the same amplitude-frequency responses.

The sensitivity to acceleration components acting in the plane perpendicular to the measured component is due to the displacement of the center of mass of the inertial element in the MSS relative to the midplanes of the elastic element plates (see Fig.38). This sensitivity can reach 15% relative to the measured component. Partial compensation for this error is achieved by installing IPTM on the wedge-shaped stand BP^{α}, the angle α between the upper and lower surfaces of which is equal to the angle between the surface of the elastic element and the plane that passes through the centers of the inertial element $\mathrm{C}i$ and the plates Cp. The error caused by these acceleration components is reduced to 3%.

The carrier also functions as a mechanical separator of the silicon IPTM, protecting it from stresses caused by the attachment of the accelerometer and deformation of the object.

The specifications of the small silicon accelerometer are as follows: dimensions $= 10 \times 8 \times 3\ mm$; weight $= 1.5\ gramm$; acceleration ranges $= 0 \pm 15\ g, 0 \pm 30\ g$; sensitivity $= 6.6\ mV/g$ and $3.3\ mV/g$; transverse sensitivity 3%; operating frequency range $= 0 \div 150$ and $0 \div 300\ Hz$; basic error $\leqslant 3\%$; operating temperature range $= -60$ to $+200^{\circ}C$; temperature compensation range $= 0 \div +200^{\circ}C$; additional components of temperature error: temperature drift of the initial output signal $< 0.04\%/^{\circ}C$, temperature sensitivity drift $< 0.04\%/^{\circ}C$; supply voltage $= 10\ V$; circuit input resistance $= 800 \div 1000\Omega$.

3. Conclusions

1. Based on the physical and functional models of IPT developed in this work and the principles of their design identified, constructions were created, prototype samples were manufactured and the metrological characteristics of the pressure and acceleration sensors were measured [6]. The obtained technical characteristics meet the requirements imposed on the elements of control, monitoring, regulation systems for research and development testing of products by the Ministry of General Machine Building.
2. Static dynamic pressure sensors ranging from $0 \div 1$ atm to $0 \div 10$ atm with dimensions of $\varnothing 13 \times 11$ and weighing less than 10 g, containing monolithic IPTs with distributed parameters without isolating $p-n$ junctions, are characterized by intrinsic error less than 1% and additional temperature error less than $0.05\ \%/^{\circ}C$ in the temperature range of $(0 \div 300)^{\circ}C$.
3. Low-frequency $(0 \div 300\text{Hz})$ acceleration sensors $(0 \pm 100 \ldots 0 \pm 300) M/c^2$ with dimensions of $10mm \times 8mm \times 3mm$ and weighing less than 2g, containing a monolithic IPT_A with an isolating $p-n$ junction, are characterized by intrinsic error of less than $\pm 5\%$ and additional temperature error from $0.06\ \%/^{\circ}C$ to $0.13\ \%/^{\circ}C$. The temperature operating range is $(0 \div 200)^{\circ}C$.

References

1. Spalek, Y. M., Kharenko, K. Yu., Suprun, S. D., Malkov, Y. V., et al. (1986). *Integral Semiconductor Pressure Transducer* (Patent No. SU1210076A1). ↩
2. Tikhomirov, M. Y., Spalek, Y. M., Morozov, Y. M., et al. (1990). *Research, development and improvement of manufacturing technology of integral transducers and sensors of energy parameters, including for control and regulation of parameters of technological processes of MEA production (Flexible manufacturing systems (FMS), Flexible manufacturing modules (FMP), etc.) Otchet o NIR [R;D report] 925.24.432-90. Manuscript in Russian.* https://doi.org/10.5281/ZENODO.7090973 ↩
3. Roylance, L., & Angell, J. (1978). A miniature integrated circuit accelerometer. *1978 IEEE International Solid-State Circuits Conference. Digest of Technical Papers*, 220–221. https://doi.org/10.1109/ISSCC.1978.1155836 ↩
4. Runyan, W. R. (1965). *Silicon Semiconductor Technology*. McGraw-Hill. ↩
5. Tikhomirov, M. Y., Spalek, Y. M., Kharenko, K. Y., et al. (1988). Issledovanie, razrabotka perspektivnykh konstruktorsko-tekhnologicheskikh reshenii, obespechivayushchikh uluchshenie metrologicheskikh ehkspluatatsionnykh kharakteristik datchikov apparatury [Research and development of promising design and technological solutions that improve the metrological and operational characteristics of instrumentation sensors]. *Otchet NIR (Zakl.) [R and D Report (Final)]*, 92522.393-89(In Russian). ↩
6. Tikhomirov, M. Y., Spalek, Y. M., Ilyashev, G. I., Zhelonkin, E. A., & Kharenko, K. Y. (1989). Ehksperimental'nye issledovaniya kharakteristik datchikov davleniya novogo pokoleniya [Experimental studies of the characteristics of the new generation of pressure sensors]. *Trudy NPO Ehnergomash*, 17(In Russian). ↩